The relationship between pumped traps and signal loss in buried channel CCDs

Conference or Workshop Item

The relationship between pumped traps and signal loss in buried channel CCDs

Neil J. Murray[1], David J. Burt[2], David Hall[1], Andrew D. Holland[1]
[1]Centre for Electronic Imaging, Open University, Milton Keynes, MK7 6AA, UK
[2]e2v technologies plc., 106 Waterhouse Lane, Chelmsford, CM1 2QU, UK

ABSTRACT

Pocket-pumping is an established technique for identifying the locations of charge trapping sites within the transport channels of CCDs. Various parameters of the pumping process can be manipulated to increase the efficiency, or allow characterisation of the trap sites effective during nominal operating modes.

A CCD273 was irradiated in a triangular region by protons to a 10 MeV equivalent fluence of 1.2E9 p.cm^{-2}, ensuring a suitably low trap density for the development of an automated trap recognition algorithm. X-rays of 5,898 eV were incident on the CCD above the region irradiated with the triangle, such that events could be analysed having passed through an increasing length of irradiated silicon and hence number of trapping sites as a function of column number.

Here we present the relationship between the number of traps identified by pocket pumping within the parallel transport channels of a CCD273 and the amount of signal that is deferred by the trapping process during readout.

Keywords: CCD, CIC, tri-level, multi-level, Euclid VIS, CTE, pocket pumping, trap pumping, EPER, FPR

1. INTRODUCTION

The aim of the experimental work described here is to demonstrate a linear relationship between the number of traps identified in the transport volume of the buried channel through trap pumping and the signal loss in charge packets that occupy that volume of the buried channel during charge transfer, *i.e.* that traps identified by pumping are responsible for CTI.

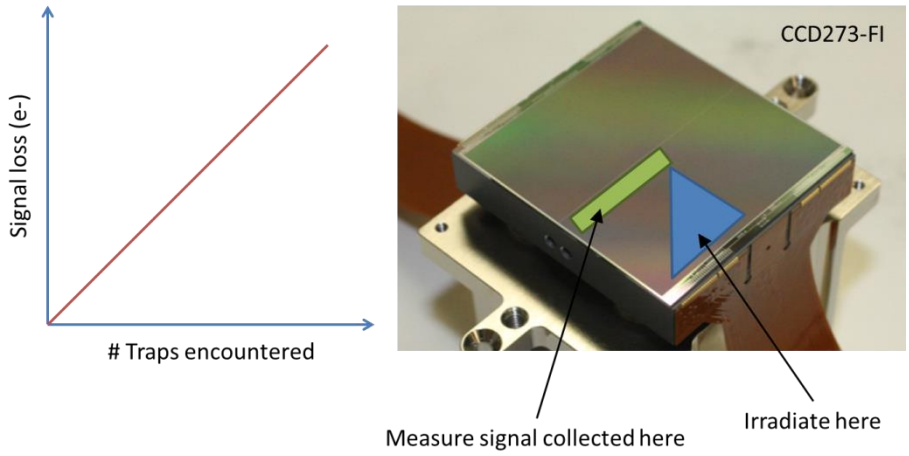

Figure 1. Left: Expected relationship between number of traps and signal loss. Right: Experimental geometries of the CCD.

*n.j.murray@open.ac.uk; tel: +44 (0)1908 332769; fax: +44 (0)1908 655910; http://www.open.ac.uk./cei

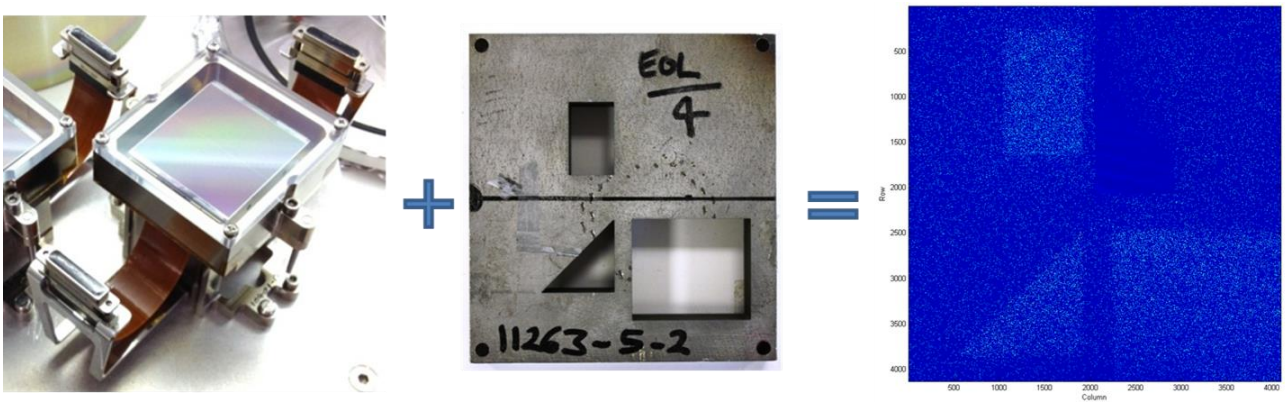

Figure 2. Irradiation of the CCD. Left: Front-illuminated CCD273. Centre: Irradiation shield. Right: Full CCD image showing pumped trap locations, showing increased trapping sites in regions exposed to protons.

A pre-development Euclid VIS CCD273 [1] was irradiated with protons to a level of 1.2 E9 p.cm-2 (10 MeV) equivalent; roughly to ¼ the expected end of life mission dose, to allow a suitably low trap density for analysis. Figure 2 shows the device, irradiation mask and resulting areas of increased trap density in the full 4k x 4k frame. The CCD was cooled to 153K, the nominal Euclid VIS operating temperature and the pixel rate used was 200 kHz. Following the Charge Transfer Efficiency (CTE) improvements for the Euclid VIS CCDs described in [2], the line transfer time was increased to 4 ms and the frame Integration time was 565 seconds. Image electrodes were biased as: Image High = 10.5 V, Image Low = 0 V, Image Very Low = -5 V.

2. TRAPS IDENTIFIED THROUGH PUMPING

Trap locations relevant to Euclid VIS readout conditions were identified by trap pumping over one cycle. This means that the background signal was transferred forward by one row, before being transferred backwards to its original location. The time taken to transfer one row in either direction is identical to that of the nominal Euclid VIS timings (4 steps of 1 ms) and the dwell time between transfers is equal to the register read time (10.5 ms). As the number of traps identified through pumping scales with the background signal, a background level of ~1,600 electrons was chosen to identify only the trap sites ^{55}Fe events may encounter during readout. Actually, the background signal was slightly larger than probe signal (^{55}Fe events) to account for depletion of the background signal during pumping.

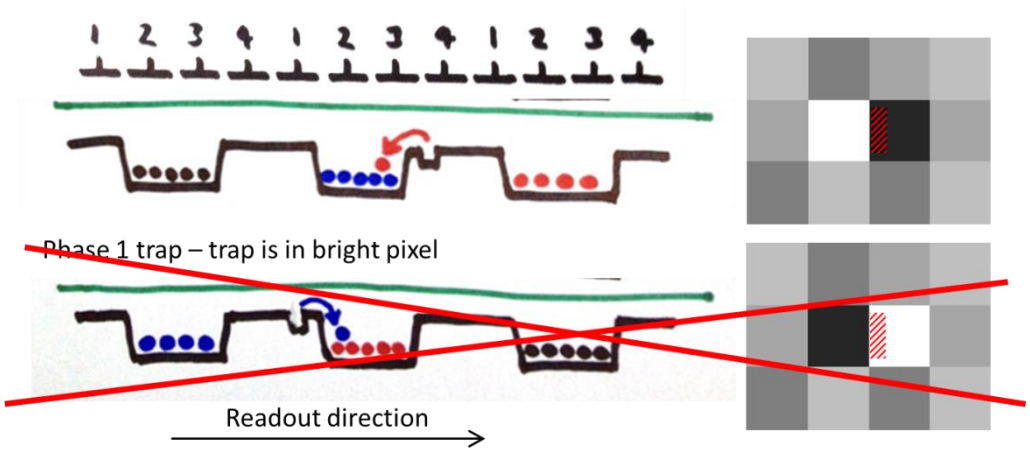

Figure 3. Trap pumping dipole orientations observed in a CCD image and the barrier phase trap locations responsible for generating them. Traps under phase one are most likely to release trapped charge back into the original charge packet and hence not counted.

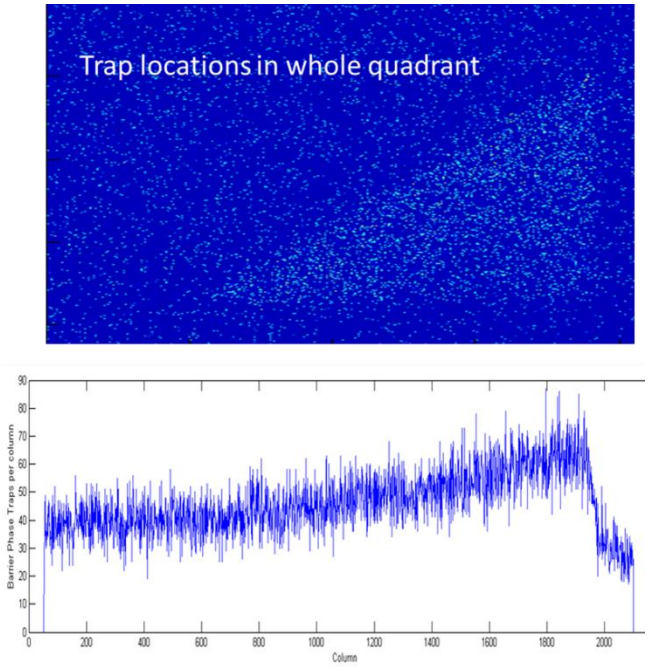

Figure 4. Trap locations and counts per column identified in triangle quadrant by trap pumping.

During the trap pumping process, signal is 'pumped' from one pixel to the next depending on both the direction of transfer and the sub-pixel location of the trap. This leads to classic dipole orientations observed in trap pumped images of dark followed by bright pixels and *vice-versa* (examples are shown in Figure 3). Only traps located under the barrier phase electrodes are efficiently pumped and as charge is only transferred in the forward direction during readout, only traps identified under the first barrier phase (4) are counted per column for the experiment – these are the CTI causing suspects. Figure 4 shows the traps identified in the quadrant of the CCD273 irradiated with the triangle pattern and the corresponding trap count as a function of column number. It should be noted that the CCD used in this experiment had failed CTE screening by e2v and so has a far higher than usual intrinsic trap density, indicated by the high trap density in the unirradiated columns.

3. X-RAY IMAGE GENERATION

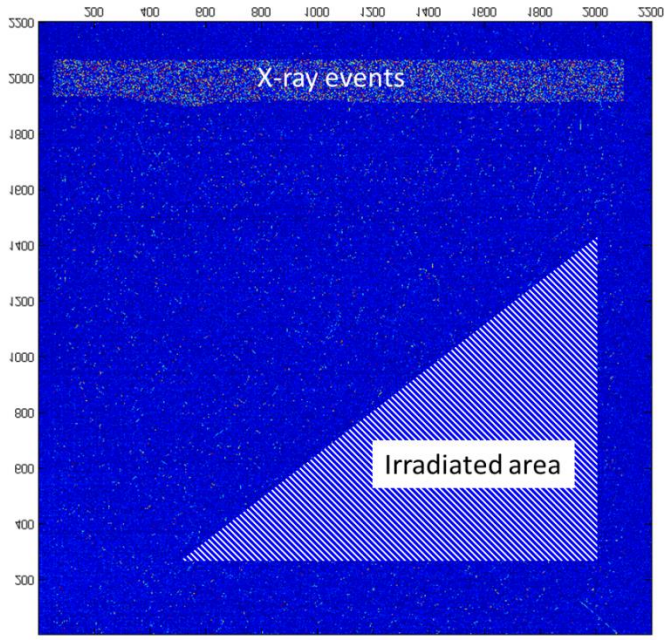

Figure 5. Example of X-ray image. Sum of 100 exposures of 565 seconds.

The CCD was shielded such that only a small area in the centre, above the triangle irradiation, was exposed to ^{55}Fe over the nominal Euclid VIS exposure time of 565 seconds. As the flux was low, 100 frames were acquired for statistical purposes.

4. X-RAY SIGNAL LOSS MEASUREMENT

For each column, a histogram was produced of the pixel data in the area exposed to ^{55}Fe events over the 100 frame dataset. Each column was then represented in a two-dimensional histogram, as shown in Figure 6. The thick lower red line indicates the background level of 0 electrons. The 1,603 electron ^{55}Fe X-ray peak is visible towards the top of the image and can be seen to shift slightly towards the background level from columns ~600 to ~1,900, corresponding to the triangle irradiation.

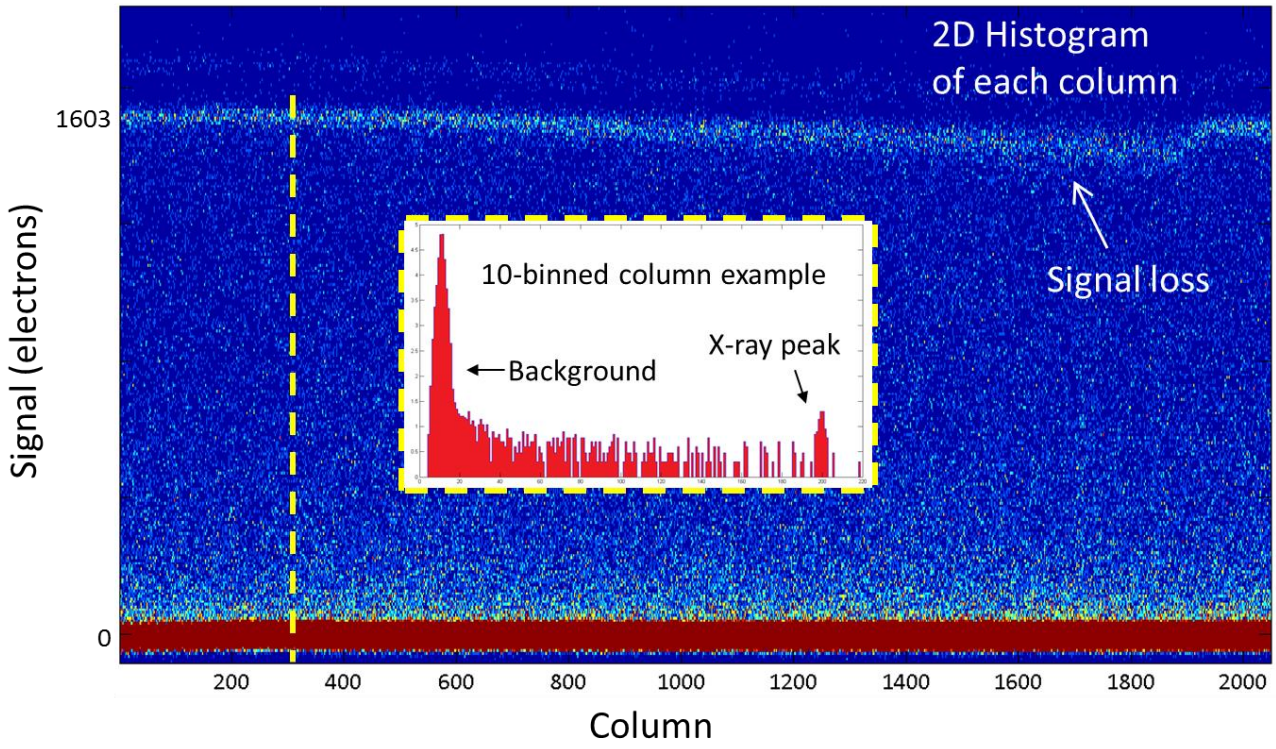

Figure 6. Two-dimensional histogram showing ^{55}Fe X-ray peak shift as a function of column number. The dashed line and box demonstrates the histogram generated from ten adjacent columns.

5. INTIAL COMPARISON OF TRAPS AND SIGNAL LOSS

The number of traps identified from trap pumping was plotted against the signal loss observed in the ^{55}Fe X-ray peak shift. The relationship was not 1:1 as expected, as shown in Figure 7 (left), with more signal being lost than could be accounted for by the number of traps observed in the trap pumped images. Additionally, no difference was observed between the data acquired with 10 µs and 1,000 µs parallel clock steps. This suggests that a significant amount of signal is being lost to trap species with a much longer emission time constant than either of the line times – referred to as 'slow' traps.

In Figure 7 (right), we see the background signal dependence as to be expected. The greater the background signal, the greater the number of traps that are identified.

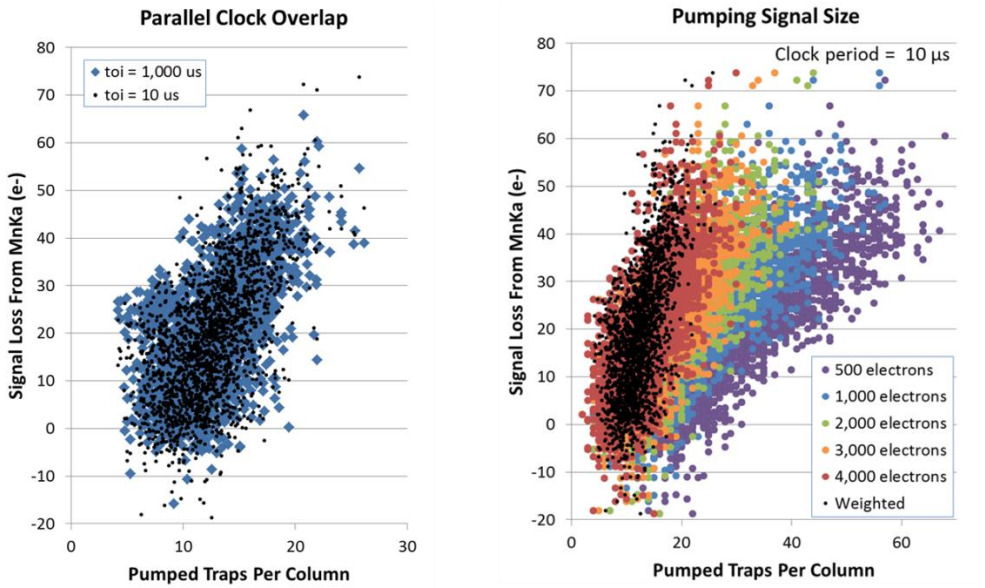

Figure 7. Initial results of Pumped Trap Count Vs. Signal Loss. Left: As a function of parallel clock overlap time (t_{oi}). Right: As a function of background signal.

6. 'SLOW' TRAPS

During detailed CTE investigations for Euclid VIS in parallel to this experiment, it was noted that although e-centre trap species had been 'frozen' out by operating the device at 153K, during the long frame integration time these traps had a reasonably high probability of becoming empty and capable of trapping significant levels of charge. Values of 1 in 4 pixels were inferred for end of life performance, initially from X-ray stack line data and then confirmed by the First Pixel Response (FPR) measurements shown in Figure 8.

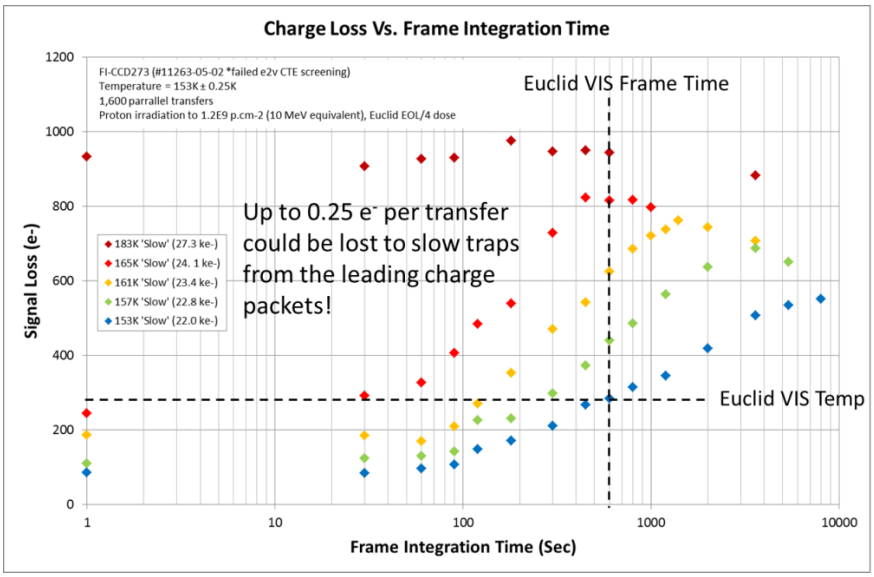

Figure 8. 'Slow' trap charge loss measurements from first pixel response measurements as a function of integration time and temperature. As the frame integration time is increased, more of the 'slow' traps are emptied and hence the larger the signal loss measured by FPR. The warmer the device, the faster the slow traps empty, causing a shift to the left of the curves.

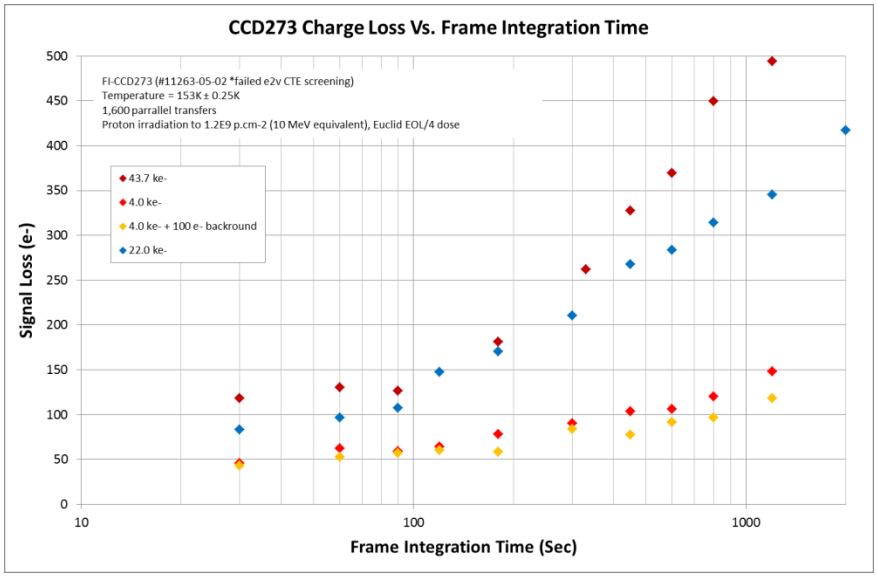

Figure 9. 'Slow' trap charge loss measurements from first pixel response measurements as a function of integration time and signal. Again as the frame integration time is increased, more of the 'slow' traps are emptied and hence the larger the signal loss measured by FPR. The greater the signal size, the larger the number of slow traps that are encountered and hence the greater the signal loss.

Any signal trapped by 'slow' traps may be released over many hundreds of seconds and is therefore unlikely to cause the classic exponential tail arising from poor CTE. Such artifacts are caused by trap species that have an emission time constant similar to the line transfer time, ≤ 4 ms. This means that 'slow' traps will not introduce smearing distortions to the galactic shapes sampled by Euclid VIS, but some signal may be lost from their leading edges. It should be noted that the cosmic ray background should mitigate 'slow' traps in the case of Euclid VIS, with periodic charge injection prior to frame integration also an option.

The locations and densities of 'slow' traps per pixel can be found by over exposing the CCD to a near infra-red flat field illumination, fast dumping the frame and then integrating a long dark exposure to collect all the electrons released from the 'slow' traps. Multi-level clocking [3] is used during the frame dump to pin the surface and eliminate any surface trap components to the persistence. In the triangle irradiated area of the CCD273, it was found that between 1 and 40 electrons could be released into individual pixels during a 565 second dark integration.

To remove the effect of 'slow' traps in the number of traps verses signal loss experiment, sacrificial charge injection was introduced into the area of the imaging array immediately before the ^{55}Fe events, to fill all these traps in the irradiated area, prior to the transfer of ^{55}Fe events through it.

7. X-RAY IMAGE GENERATION WITH CIC BIAS

Bias rows of ~6,000 electrons were injected into the imaging array using the Clock Induced Charge (CIC) method described in [3], between the area exposed to ^{55}Fe X-ray photons and the triangle irradiated area. The CIC background fills the entire imaging area and so is initially clocked forward a few rows into the dump drain and then clocked backwards to the central charge injection drain, leaving only 200 rows of bias signal in the array. This is the clocked forward into the desired location before the 565 second integration of ^{55}Fe X-rays. The forward and backward parallel transfer timings are equal and the same as those used during the readout of the frame. This allows for EPER measurements to made on both edges of the bias signal.

Similar to Figure 5, Figure 10 shows the result of 100 stacked frames acquired by this method. This time the 'slow' traps in the triangle area irradiated by protons are completely filled before the X-ray events would have encountered them during readout.

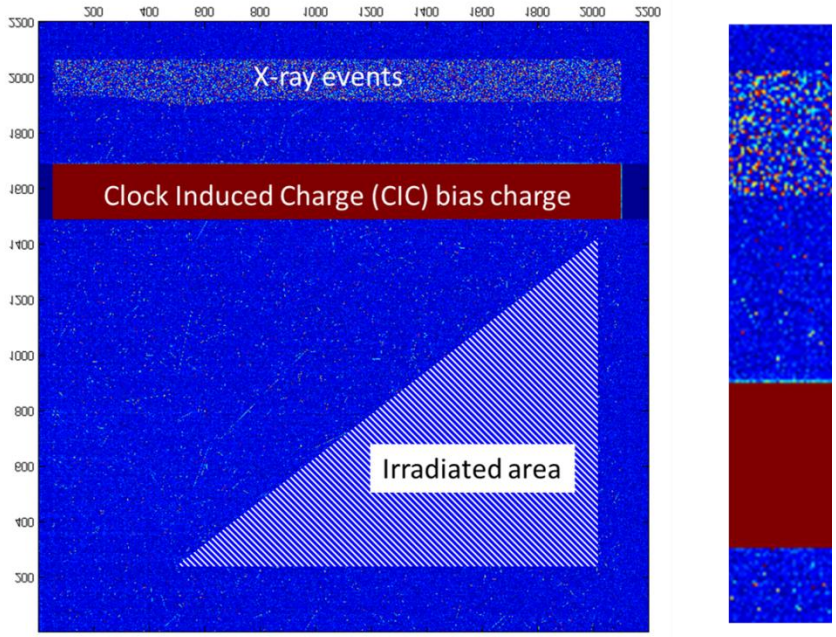

Figure 10. Example of X-ray image including CIC bias to fill slow traps. Sum of 100 exposures of 565 seconds.

8. X-RAY SIGNAL LOSS MEASUREMENT WITH CIC BIAS

Histograms of the pixel data for each column in the ^{55}Fe exposed area were produced for the 100 frame dataset and each column was then represented in a two-dimensional histogram, as shown in Figure 11. The thick lower red line indicates the background level of 0 electrons. The 1,603 electron ^{55}Fe X-ray peak is again visible towards the top of the image and this time can be seen to have less of a shift towards the background level between columns ~600 to ~1,900, as was seen in Figure 6. The two ^{55}FE signal loss regions of both Figures 6 and 11 are compared in Figure 12, demonstrating the improvement in signal loss by the CIC bias charges.

It was however found that 100 frames in the dataset were not sufficient to accurately provide a measurement of signal loss for each column. Due to the long exposure time (565 seconds), it was not practicable to increase the sample size simply by acquiring more data. The EPER and FPR of the bias charge introduced into each frame was analysed to see if it could be used to measure both the 'fast' and 'slow' trap losses in a more efficient manner.

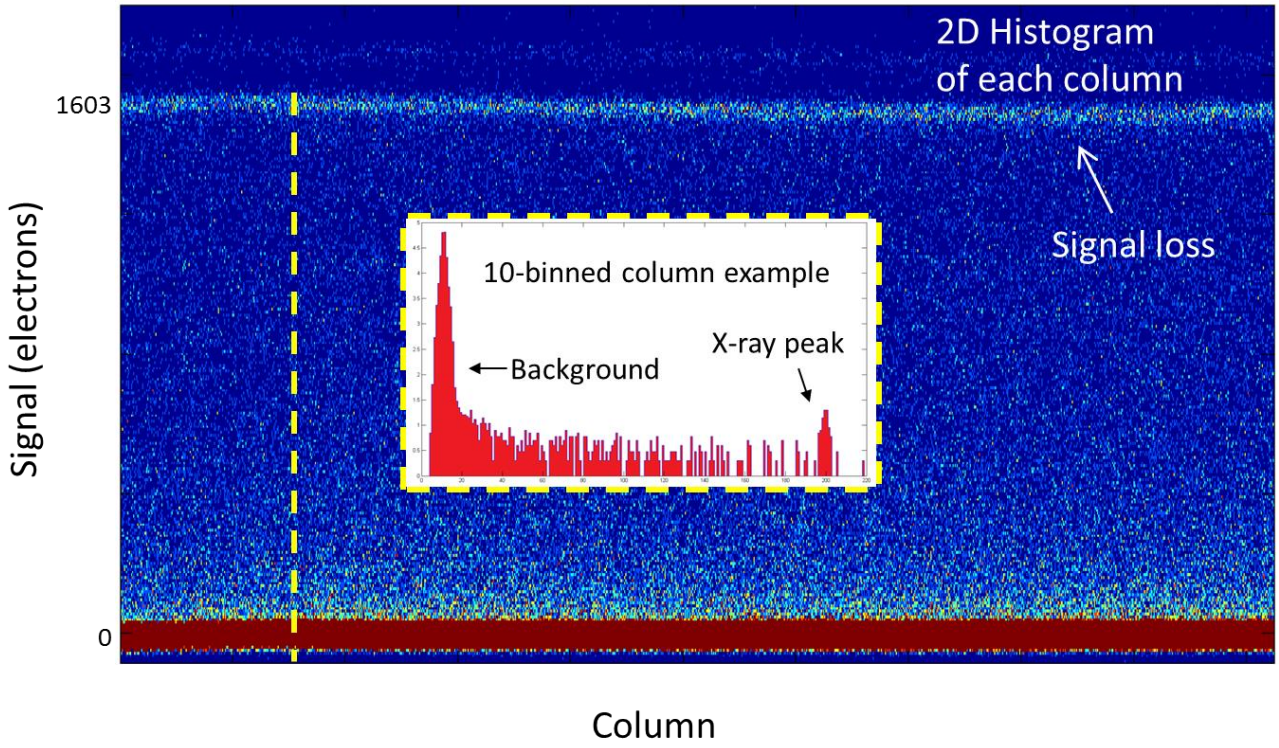

Figure 11. Two-dimensional histogram showing reduced ^{55}Fe X-ray peak shift as a function of column number due to the introduction of bias charge to fill 'slow' traps. The dashed line and box demonstrates the histogram generated from ten adjacent columns.

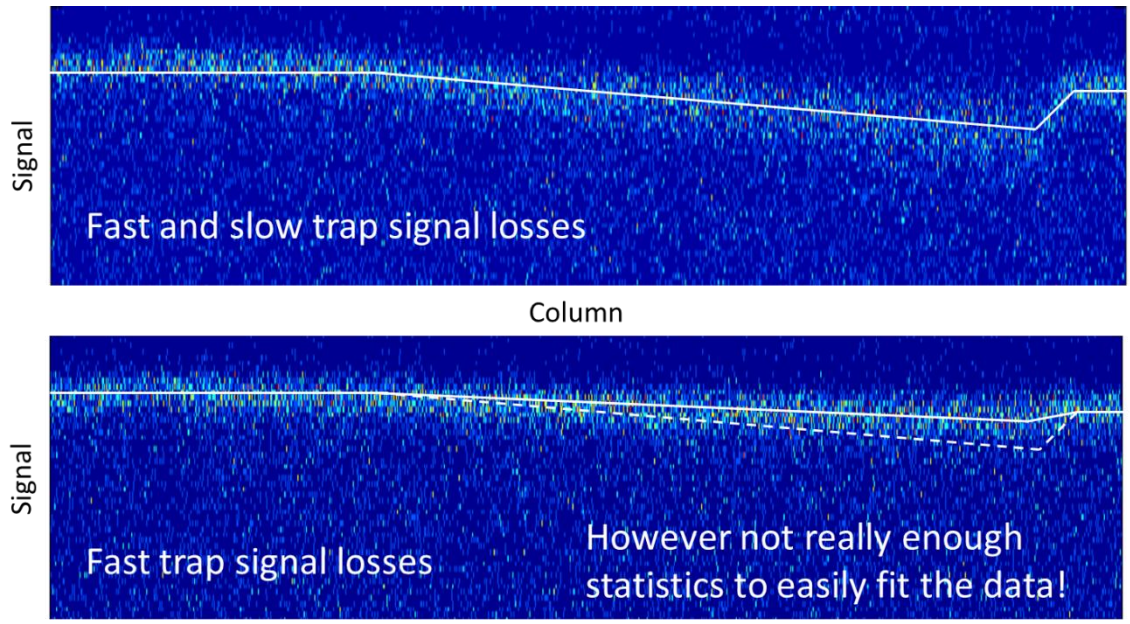

Figure 12. Comparison of 55Fe X-ray event signal losses when transferred through the triangle irradiated region with (lower) and without (upper) 6,000 electrons bias preceding the signal. The biased data show signal losses as a result of 'fast' traps only, whereas the unbiased data show 'fast' and 'slow' trap contributions.

9. FIRST PIXEL / EXTENDED PIXEL EDGE RESPONSE MEASUREMENTS

The measurements shown in Figures 8 and 9 were obtained from an area in the opposite half of the CCD273. The rectangular irradiation pattern is shown in Figure 13. Again, a uniform block of bias was injected by manipulating CIC and then held for 565 seconds before being read out. The manipulation of the position of the bias charge was as per the read out timings, such that representative EPER measurements could be obtained to measure the signal deferred by 'fast' traps. The leading edge of the bias charge was analysed by the FPR method to measure the 'slow' trap losses.

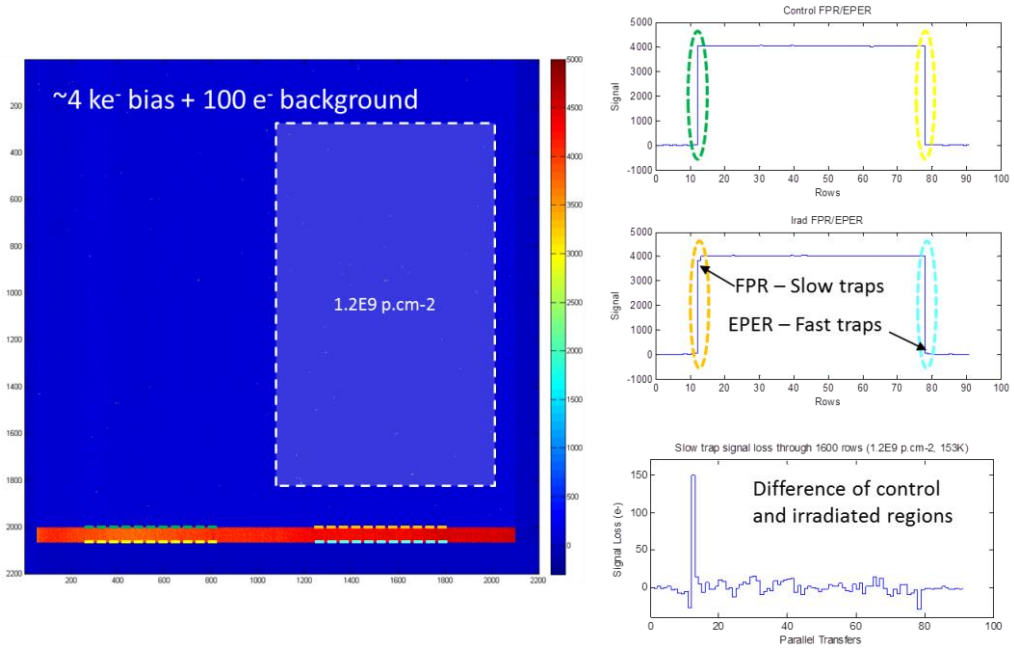

Figure 13. Example image used to measure 'fast' and 'slow' trap effect on 4,000 electrons signal.

Figure 14 shows the contributions of both the 'fast' and 'slow' traps to signal loss in the quadrant of the CCD273 irradiated with the triangle pattern. Here we can see that the 'slow' traps dominate and this is no surprise as the parallel transfer was optimised in [2] to significantly reduce the effect of 'fast' traps.

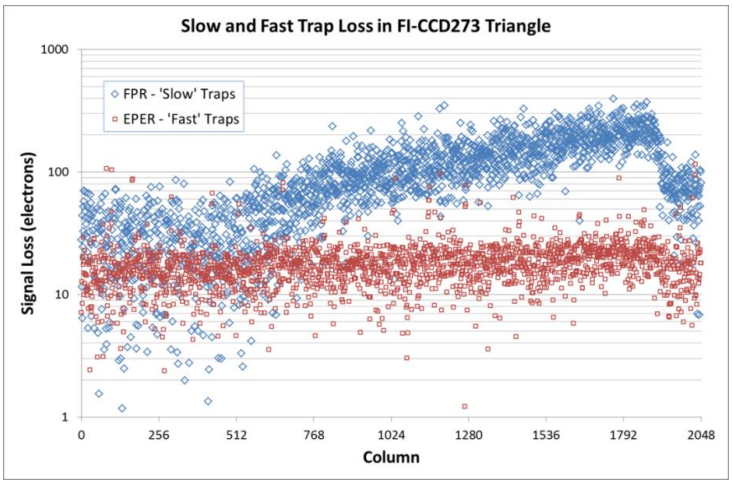

Figure 14. 'Fast' and 'Slow' trap contributions to charge loss as a function of column number in triangle irradiated quadrant.

10. RESULTS

Figure 15 shows both the 'fast' and 'slow' trap signal loss data plotted against the number of traps identified in their respective columns. As the bias signal used for the measurement (6,000 e^-) was at a larger level than the original ^{55}Fe (1,603 e^-), a larger background signal was required for pumping to identify the 'fast' trap count.

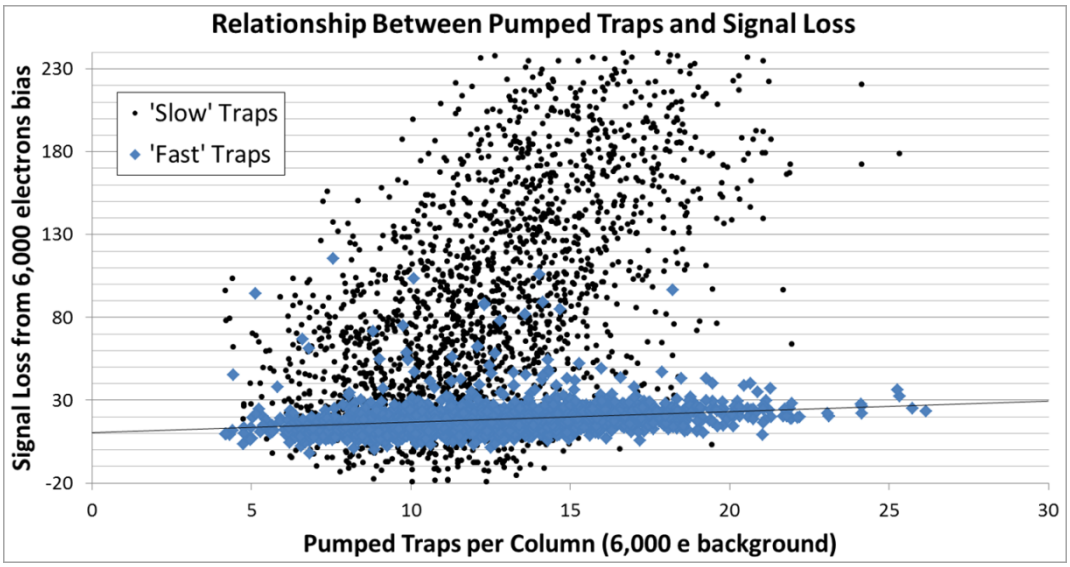

Figure 15. The relationship between pumped traps and signal loss in buried channel CCDs with a linear fit to the 'fast' trap data.

Removing the 'slow' trap component, we now see a roughly 1:1 relationship between the number of traps identified through trap pumping and the signal loss/deferred into subsequent pixels.

11. CONCLUSIONS

Schemes were presented for probing 'fast' and 'slow' traps species that will be present in the Euclid VIS during the mission. Two-dimensional histograms showed the effect of the triangular irradiation on signal transferred through it. Initial comparison of total traps counted per column against the signal loss in that column showed that more signal was being lost than expected due to the larger number of 'slow' traps. An area of CIC bias signal was introduced to fill 'slow' traps before the X-ray events passed through the irradiated region, significantly improving the performance. Due to limited X-ray statistics, the EPER of the bias charge was used to characterise the 'fast' traps. Removing the 'slow' traps leaves a reasonable 1:1 relationship between the number of traps identified by pumping in a single column to the signal loss as the charge packet is transferred through that column.

REFERENCES

[1] Endicott, J., *et al*., "Charge-coupled devices for the ESA Euclid M-class Mission", Proc. of SPIE, Vol. 8453 (2012).

[2] Murray, N. J., *et al*, "Mitigating radiation-induced charge transfer inefficiency in full-frame CCD applications by 'pumping' traps", Proc. of SPIE, 845317 (2012).

[3] Murray, N. J., *et al*, "Multi-level parallel clocking of CCDs for: improving charge transfer efficiency, clearing persistence, clocked anti-blooming and generating low noise backgrounds for pumping", Proc. of SPIE, 886020 (2013).